Available online at www.sciencedirect.com
SCIENCE DIRECT®
ELSEVIER
International Journal of Multiphase Flow 31 (2005) 263–284
International Journal of Multiphase Flow
www.elsevier.com/locate/ijmulflow

Gas absorption into a drop in the presence of an acoustic field

A. Muginstein, M. Fichman, C. Gutfinger *

Faculty of Mechanical Engineering, Technion—Israel Institute of Technology, Haifa, Israel

Received 13 August 2003; received in revised form 1 November 2004

Abstract

The present work considers acoustically enhanced gas absorption into a liquid drop accompanied by a homogeneous first order chemical reaction.

The mass conservation equation was solved for the flow inside the drop induced by acoustic streaming both analytically and numerically. Two cases were considered: An analytical solution was presented for the case of high Peclet numbers, while the case of arbitrary Peclet numbers was solved numerically.

The high Peclet number case is applicable for high circulation rates and serves as an upper limit on the rate of mass transfer into the drop. It also provides a check for the numerical solution.

The results indicate that the effect of the acoustic field on mass transfer is especially beneficial for absorption processes without chemical reaction, or with reactions of moderate rates. The enhancement for these processes for Peclet numbers of 500–1000 was 3.3–3.5 as compared to absorption without an acoustic field. For processes with fast chemical reactions the benefits of using an acoustic field are limited, with enhancement factors in the range of 1.5–2.3.

Keywords: Gas absorption; Acoustics; Drops; Diffusion; Convection; Internal circulation

* Corresponding author.
E-mail address: gutfinge@techunix.technion.ac.il (C. Gutfinger).

0301-9322/$ - see front matter © 2004 Elsevier Ltd. All rights reserved.
doi:10.1016/j.ijmultiphaseflow.2004.11.007

1. Introduction

Oscillatory flows are of increasing interest in the enhancement of heat and mass transfer. When a sound wave is applied to a fluid, steady motion known as acoustic streaming may take place under certain conditions. Consider a sphere or a cylinder immersed in the oscillating fluid, when the amplitude of the oscillation is small as compared to the characteristic length of the sphere or cylinder. Under such conditions a steady motion will take place around the body. The streaming around the body is confined to what is known as an acoustic boundary layer, the thickness of which is of the order of $O(v_0/\omega)^{1/2}$.

Schlichting (1979) considered streaming flow around an oscillating cylinder. This work explained an observation made by Andrade (1931) regarding vortices generated by an oscillating cylinder in a water tank. Lane (1956) and Raney et al. (1955) studied theoretically and experimentally the acoustic streaming around a rigid sphere and cylinder, respectively. Theoretical studies were also conducted by Riley (1966), Burdukov and Nakoryakov (1965a,b), Wang (1965), Stuart (1966) and Lee and Wang (1988, 1989). A recent review published by Riley (1997) describes different types of acoustic streaming.

The effect of oscillating flow on heat and mass transfer was already acknowledged more than 60 years ago. Since then substantial research effort has been devoted to this topic.

Marthelli and Boelter (1939) reported that heat transfer from a vibrating cylinder is five times higher than that from a stationary cylinder in free convection. Lemlich and Rao (1965) found a fourfold increase in free convection heat transfer from vibrating wires as compared to non-vibrating ones. Baxi and Ramachandran (1969) studied the effect of vibration on natural and convective heat transfer. While enhancement was observed in natural convection, it was practically non-existent under forced convection conditions. Mori et al. (1969) studied heat transfer from small spheres at low Strouhal numbers, finding no effect on the heat transfer rate. Larsen and Jensen (1978) studied experimentally the effect of flow pulsation on the evaporation rate from a sphere at high Strouhal numbers with and without forced convection, reporting an up to 90% increase in evaporation rate. Ha and Yavuzkurt (1993) performed a numerical investigation to assess the effect of a high intensity acoustic field on heat and mass transfer from solid particles and droplets. Nasiri and Van Moorhem (1996) studied the sublimation rate from solid spheres using low frequency pulsation. Yarin et al. (1999) studied theoretically and experimentally the streaming patterns of an acoustically levitated drop accounting for effects of compressibility and modification of droplet shape due to acoustic pressure. From the streaming patterns evaporating rates were calculated. The same theory was applied to estimate the sublimation rate from a solid sphere (Yarin et al., 2000).

Although considerable effort has been invested in the study of heat and mass transfer in the presence of acoustic fields, most of the works deal with the effect of acoustic streaming on heat or mass transfer external to the bodies considered, and little work has been devoted to the effect of internal flow, brought about by the external streaming motion on heat and mass transfer, where the internal resistance to these processes is dominant. This situation has relevance in many industrial processes such as scrubbing, absorption and waste gas purification.

The liquid inside the drop is driven by the gas flow near the drop surface and therefore affects mass transfer inside the drop. Although, Yarin et al. (1999) concluded that internal flow has a negligible effect on mass transfer dominated by external resistance, such as evaporation from a

liquid drop, we will show that it cannot be neglected when the resistance to mass transfer is in the dispersed phase, such as in the case of gas absorption into a liquid drop.

Another class of works deals with internal flows generated by acoustic waves (Vainshtein et al., 1995; Larsen and Jensen, 1978). These works are characterized by the existence of a hydrodynamic boundary layer near the surfaces. The thickness of this boundary layer is of the order of $Pe^{-1/2}$. Usually, in this kind of boundary layer problems one should consider for this region a separate slow timescale solution for the net diffusion across the streamlines. Examples of such problems are the flow around a solid sphere, dissolution or growth of spherical oscillating bubbles (Fyrillas and Szeri, 1994), and diffusion in Rayleigh–Bennard cells and spatially periodic flows (Young et al., 1989; Rosenbluth et al., 1987; Rhines and Young, 1983). Our problem is different in the fact that in our case the velocity at the boundary is maximal, while in those cases it is either minimal or zero. Hence, in our case there is no thin boundary layer near the gas–liquid interface, where the velocity develops.

In the present work, we study the effect of internal circulation caused by the streaming flow outside the droplet on mass transfer into the droplet with or without chemical reaction. Analytical and numerical solutions are presented, and practical conclusions are drawn.

2. Flow field in the presence of an acoustic field

We now present the governing equations for acoustical streaming near spherical drops and further on, the equation for the induced internal flow inside the drop. In this section, we use arguments similar to those in the work of Burdukov and Nakoryakov (1965b) for evaluating the velocity outside the drop. The internal flow is calculated using similar assumptions to those of Yarin et al. (1999).

We consider a spherical drop immersed in a fluid perturbed by an acoustic field, and make the following assumptions:

1. The drop remains spherical.
2. Large Strouhal number, S,

$$S = \frac{\omega a}{B} \gg 1 \tag{1}$$

where B, ω and a are respectively the velocity amplitude, fluctuation frequency and drop radius.

$$B = \frac{A_0}{\rho_0 c_0} \tag{2}$$

A_0, ρ_0 and c_0 are, respectively, the sound pressure, continuous phase density and isentropic sound velocity.

3. Large acoustic Reynolds number

$$Re_s = \frac{\omega a^2}{v_0} \gg 1 \tag{3}$$

where v_0 is the continuous phase viscosity.

Under these assumptions, a steady secondary flow will develop near the droplet surface, which can be expressed as:

$$\langle u \rangle = \Gamma(x,y) + \varphi(x)y + \beta(x) \tag{4}$$

The first term in Eq. (4) is the velocity around a rigid sphere obtained by Burdukov and Nakoryakov (1965b). Note that $\Gamma(x,y)_{y=0} = 0$ implies that $\beta(x)$ is the fluid velocity on the drop surface. Moreover, as the fluid is stagnant far from the drop surface, we obtain that $\varphi(x) = 0$.

To simplify the solution inside the drop we assume that the inertia terms are negligible as compared to the viscous terms. This leads to the well-known creeping flow equation:

$$\mathrm{D}^4\psi_i = 0 \tag{5}$$

The solution of Eq. (5) is:

$$\psi_i = E\left(\frac{R^3}{a} - \frac{R^5}{a^3}\right)\sin(\theta)\sin(2\theta) \tag{6}$$

where R and θ are the radial and angular coordinates, respectively.

Matching velocities and shear stresses between the external solution of Eq. (4) and the internal solution of Eq. (6) eliminates the constant E in Eq. (6) and $\beta(\tilde{x})$ in Eq. (4).

$$\psi_l = \frac{9}{160\sqrt{2}}a^2 B\frac{\mu_0}{\mu_i}S^{-1}Re_s^{-\frac{1}{2}}\left[\left(\frac{R}{a}\right)^3 - \left(\frac{R}{a}\right)^5\right]\sin(\theta)\sin(2\theta) \tag{7}$$

The induced internal flow is illustrated in Fig. 1.

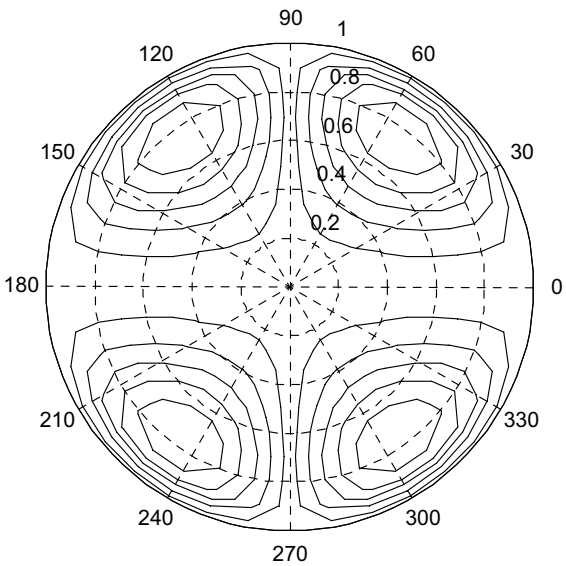

Fig. 1. Stream lines inside a drop in the presence of an acoustic field.

A similar flow pattern exists when an immersed drop in a dielectric fluid is subjected to an electric field. This pattern was predicted and observed by Taylor (1966). A similar flow pattern was also reported in the work of Stone et al. (1991). This work describes in terms of chaotic stream lines the flow inside drops, which are immersed in a bounded steady Stokes flow.

Eq. (7) is used in the next section to solve the concentration profile inside the drop and the related mass transfer rate.

3. Mass transfer into a drop

3.1. Problem formulation

Acoustic pressure influences the internal flow, thus affecting the mass transfer rate into the drop. Since the acoustic pressure does not appear explicitly in the momentum and mass conservation equations, it is more convenient to use another characteristic parameter, namely the amplitude velocity B. The characteristic velocity is related to the acoustic pressure as (Ha and Yavuzkurt, 1993):

$$B = \sqrt{2}\frac{10^{L_p-94/20}}{\rho_0(\gamma\Re T_0)^{1/2}} = \frac{A_0}{\rho_0 c_0} \tag{8}$$

where L_p is the acoustic pressure in dB, $\Re$ is the universal gas constant, and ρ_0, T_0 are the continuous phase density and temperature, respectively. Note that this characteristic velocity appears in the solution for the stream line of Eq. (7).

The mass conservation equation and the boundary conditions for an axisymmetric drop with a first order chemical reaction are:

$$\begin{aligned}
&\frac{\partial c}{\partial t} + \upsilon_r\frac{\partial c}{\partial R} + \frac{\upsilon_\theta}{R}\frac{\partial c}{\partial \theta} = D\left(\frac{\partial^2 c}{\partial R^2} + \frac{2}{R}\frac{\partial c}{\partial R}\right) + \frac{1}{R^2\sin\theta}\frac{\partial}{\partial\theta}\left(\sin\theta\frac{\partial c}{\partial\theta}\right) + k_r c \\
&c = 0 \quad @\ t = 0; \qquad \frac{\partial c}{\partial\theta} = 0 \quad @\ \theta = 0,\pi \ \ t > 0 \\
&\frac{\partial c}{\partial R} = 0 \quad @\ R = 0,\ t > 0; \qquad c = c_0 \quad @\ R = a \ \ t > 0
\end{aligned} \tag{9}$$

The velocity components υ_r, υ_θ are derived directly from the stream function of Eq. (7):

$$\begin{aligned}
\upsilon_r &= \frac{1}{R^2\sin\theta}\frac{\partial\psi_i}{\partial\theta} = 2Z\frac{R}{a^3}\left(1 - \left(\frac{R}{a}\right)^2\right)(3\cos^2\theta - 1) \\
\upsilon_\theta &= -\frac{1}{R\sin\theta}\frac{\partial\psi_i}{\partial R} = -Z\frac{R}{a^3}\left(3 - 5\left(\frac{R}{a}\right)^2\right)\sin 2\theta \\
Z &= \frac{9}{160\sqrt{2}}Ba^2\frac{\mu_0}{\mu_i}S^{-1}Re_s^{-\frac{1}{2}}
\end{aligned} \tag{10}$$

Eq. (9) in dimensionless form is:

$$\begin{aligned}
&\frac{\partial C}{\partial \tau}+\frac{1}{2}Pe\left[\frac{\widetilde{v}_\theta}{r}\frac{\partial C}{\partial \theta}+\widetilde{v}_r\frac{\partial C}{\partial r}\right]=\frac{\partial^2 C}{\partial r^2}+\frac{2}{r}\frac{\partial C}{\partial r}+\frac{\cot\theta}{r^2}\frac{\partial C}{\partial \theta}+\frac{1}{r^2}\frac{\partial^2 C}{\partial \theta^2}+Da\,C\\
&C=0 \quad @\ \tau=0; \qquad \frac{\partial C}{\partial \theta}=0 \quad @\ \theta=0,\pi/2\\
&\frac{\partial C}{\partial r}=0 \quad @\ r=0; \qquad C=1 \quad @\ r=1\\
&C=\frac{c-c_0}{c_0}, \quad \tau=\frac{D}{a^2}t, \quad r=\frac{R}{a}, \quad Da=\frac{k_r a^2}{D}, \quad Pe=\frac{Ba}{D}, \quad \widetilde{v}_r=\frac{v_r}{B}, \quad \widetilde{v}_\theta=\frac{v_\theta}{B}
\end{aligned} \tag{11}$$

Here r is the dimensionless radial coordinate; C and τ, the dimensionless concentration and time, respectively; and $\widetilde{v}_r$ and $\widetilde{v}_\theta$, the dimensionless radial and circumferential components of velocity, respectively. The process is also governed by two dimensionless groups: *Da*—the so-called Damköhler number, which gives the ratio between the reaction and diffusion rates, and *Pe*—the Peclet number, which provides a measure of the relative importance of mass transfer by acoustic convection and diffusion.

From Eq. (11), we may identify three cases:

Case 1: $Pe=0$, which represents absorption by a stagnant drop, i.e., without an acoustic field. This case has a well-known solution and we will use it to compare with it the absorption enhancement caused by the acoustic field.

Case 2: $Pe\to\infty$. This case represents absorption with strong circulation caused by the acoustic field. Here the circulation rate is faster than the solute diffusion rate into the drop. Therefore, we can neglect the diffusion along the streamlines and assume that the solute concentration on a given streamline is constant. With this approximation, an analytical solution is possible.

Case 3: Arbitrary Peclet number. Here, we cannot neglect the diffusion along the streamlines, and consequently an analytical solution cannot be obtained. Here, a numerical solution is obtained for several Peclet numbers and compared with the analytical solutions for a stagnant drop ($Pe=0$) and that with strong circulation, $Pe\to\infty$.

3.2. Case 1—Absorption into a stagnant drop with and without chemical reaction

The mass transfer equation and the boundary conditions for this case are:

$$\begin{aligned}
&\frac{\partial C}{\partial \tau} = \left(\frac{\partial^2 C}{\partial r^2} + \frac{2}{r}\frac{\partial C}{\partial r}\right) + Da\, C \\
&C = 1 \quad @\ \tau = 0 \\
&\frac{\partial C}{\partial r} = 0 \quad @\ r = 0,\ \tau > 0 \\
&C = 0 \quad @\ r = 1,\ \tau > 0
\end{aligned} \tag{12}$$

The solution without chemical reaction is,

$$C(r,\tau) = 1 - \frac{2}{r}\sum_{n=1}^{\infty} \frac{(-1)^{n+1}}{n\pi} \exp(-n^2\pi^2\tau)\sin(n\pi r) \tag{13}$$

Danckwerts (1951) modified this solution to account for a first order chemical reaction by using the following relation between the solution for the concentration without chemical reaction, C, and the concentration with, $\widetilde{C}$ with,

$$\widetilde{C}(r,t) = Da\int_0^t Ce^{-Da\,\tau}\,\mathrm{d}\tau + Ce^{-Da\,\tau} \tag{14}$$

3.3. Case 2—Absorption into a drop at high Peclet number

This case represents absorption with very strong circulation, allowing us to neglect the diffusion along the streamlines and assume that the solute concentration on a given streamline is constant.

We solve this problem by rewriting the equation of mass conservation in a streamline curvilinear coordinate system. Neglecting diffusion along streamlines, we transform the unsteady diffusion–convection Eq. (11) into an unsteady diffusion equation using the curvilinear coordinate system ψ–η (Levich, 1962; Kronig and Brink, 1950), where ψ is the streamline coordinate and η is a coordinate orthogonal to ψ. We define ψ as:

$$\begin{aligned}
&\psi = Ar^3(1-r^2)\sin(\theta)\sin(2\theta) \\
&r = \frac{R}{a}, \quad A = 7,\ 0 \leqslant r \leqslant 1,\ 0 \leqslant \psi \leqslant 1
\end{aligned} \tag{15}$$

Note that ψ differs from the stream function of Eq. (7) in the multiplier A, which was set as $A = 7$ to normalize ψ. We obtain the coordinate η using the orthogonality condition:

$$\begin{aligned}
&\nabla\eta\cdot\nabla\psi = 0 \\
&\frac{\partial\psi}{\partial r}\frac{\partial\eta}{\partial r} + \frac{1}{r^2}\frac{\partial\psi}{\partial\theta}\frac{\partial\eta}{\partial\theta} = 0
\end{aligned} \tag{16}$$

which yields an expression for η

$$\eta = \frac{r^{10}}{(3-5r^2)^2}(3\cos^2\theta - 1)^5 \tag{17}$$

Fig. 2 shows an infinitesimal volume element in the streamline coordinate system.

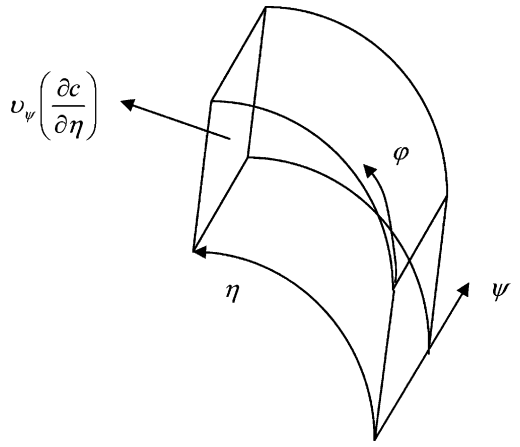

Fig. 2. Volume element in the ψ–η coordinate system.

We now rewrite Eq. (11) using the simplifying assumption of constant solute concentration along ψ,

$$\left(\frac{\partial C}{\partial \eta}\right)_\psi = 0 \tag{18}$$

In the new ψ–η curvilinear coordinate system, the mass conservation equation reads,

$$G(\psi)\left(\frac{\partial C}{\partial \tau} + Da\, C\right) = \frac{\partial}{\partial \psi}\left(\frac{\partial C}{\partial \psi} F(\psi)\right) \tag{19}$$

where $G(\psi)$ and $F(\psi)$ are:

$$G(\psi) = \int_\eta \frac{1}{h_\psi h_\eta h_\varphi}\,\mathrm{d}\eta, \quad F(\psi) = \int_\eta \frac{h_\psi}{h_\eta h_\varphi}\,\mathrm{d}\eta \tag{20}$$

and h_ψ, h_η, and h_φ are the metric coefficients,

$$\begin{aligned} h_\psi &= |\nabla \cdot \psi| = \sqrt{\left(\frac{\partial \psi}{\partial r}\right)^2 + \frac{1}{r^2}\left(\frac{\partial \psi}{\partial \theta}\right)^2} = 2A\,\Delta r^2 \sin\theta \\ \Delta &= \sqrt{(1-r^2)^2(3\cos^2\theta - 1)^2 + (3-5r^2)^2 \sin^2\theta \cos^2\theta} \end{aligned} \tag{21}$$

$$h_\eta = |\nabla \cdot \eta| = \sqrt{\left(\frac{\partial \eta}{\partial r}\right)^2 + \frac{1}{r^2}\left(\frac{\partial \eta}{\partial \theta}\right)^2} = \frac{30 r^9}{(3-5r^2)^3}(3\cos^2\theta - 1)^4 \Delta \tag{22}$$

$$h_\varphi = |\nabla \cdot \varphi| = \sqrt{\left(\frac{\partial \varphi}{\partial r}\right)^2 + \frac{1}{r^2}\left(\frac{\partial \varphi}{\partial \theta}\right)^2} = \frac{1}{r \sin\theta} \tag{23}$$

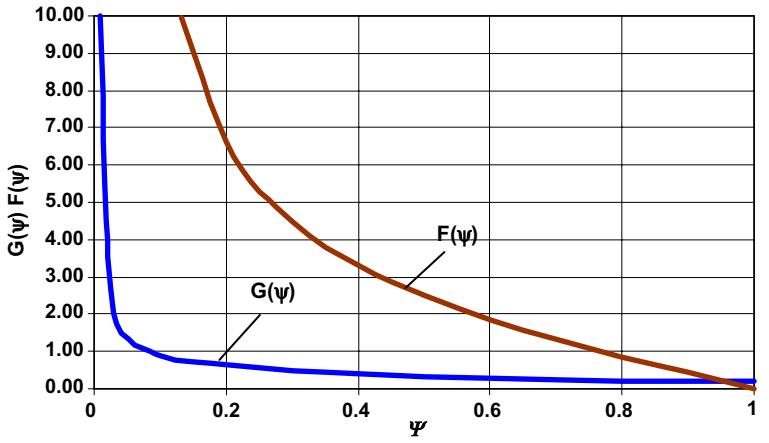

Fig. 3. Functions $G(\psi)$ and $F(\psi)$.

The functions $G(\psi)$ and $F(\psi)$, which were obtained by numerical integration of Eq. (20), are presented in Fig. 3.

To solve Eq. (19) we first consider the case of no chemical reaction and then with the help of the transformation of Eq. (14) extend the solution to the case of diffusion with a first order chemical reaction.

Eq. (19) for the case of no chemical reaction is:

$$G(\psi)\frac{\partial C}{\partial \tau} = \frac{\partial}{\partial \psi}\left(\frac{\partial C}{\partial \psi}F(\psi)\right) \tag{24}$$

with initial and boundary conditions,

$$C = 1, \quad \tau = 0$$
$$C = 0, \quad \psi = 0$$
$$C = \text{finite}, \quad \psi = 1$$

Solution for such problems is obtained by using asymptotic expansion methods, as described in Wyllie (1995).

The solution of Eq. (24) is:

$$C(\psi,\tau) = 1 - \sum_{n=1}^{\infty} E_n \Psi_n(\psi)\exp(-\lambda_n \tau) \cong 1 - E_1\Psi_1\exp(-\lambda_1\tau) - E_2\Psi_2\exp(-\lambda_2\tau) \tag{25}$$

where ψ_n and λ_n are the eigenfunctions and eigenvalues respectively, E_n is obtained from the initial condition, and,

$$\begin{aligned} &\lambda_1 = 31.935, \ \lambda_2 = 113.444 \\ &\Psi_1 = 2.6855\psi + 1.0779\psi^2 \\ &\Psi_2 = -10.9844\psi + 15.4547\psi^2 \\ &E_1 = 0.4799, \ E_2 = -0.2787 \end{aligned} \tag{26}$$

The solution for absorption with a chemical reaction is derived from Eq. (24) using the transformation of Eq. (14), to yield,

$$\widetilde{C}(\psi,t)=1-\sum_{n=1}^{\infty}\frac{E_n\Psi_n(\psi)}{\lambda_n+Da}[1+(\lambda_n+Da-1)\exp(-\tau(\tau_n+Da))] \tag{27}$$

The average solute concentration is given by:

$$C_{\mathrm{avg}}=\frac{1}{V}\int\int\int C\,\mathrm{d}s_\psi\,\mathrm{d}s_\eta\,\mathrm{d}s_\varphi=\frac{3}{2}\int_\psi CG(\psi)\,\mathrm{d}\psi \tag{28}$$

The solutions given in Eqs. (25) and (27) are valid when $Pe\to\infty$. This is a limiting case, which disregards the change in concentration along the streamlines, as indicated by Eq. (18). In practice, this means that the rate of circulation is fast enough, such that the change in concentration along the streamline due to crosswise mass diffusion toward it can be neglected.

Typically, problems of this kind are usually treated by dividing them into two domains, a thin layer near the boundary and a core region. Examples may be problems that deal with internal flows generated by acoustic waves (Vainshtein et al., 1995; Larsen and Jensen, 1978). These works are characterized by the existence of a hydrodynamic boundary layer near the surface, the thickness of this which is of the order of $Pe^{-1/2}$. Usually, in that kind of boundary layer problems one should consider a separate slow timescale solution for the net diffusion across the streamlines inside the boundary layer. Our problem is different in the fact that here the velocity at the boundary, i.e., at the air–liquid interface is maximal, while in the internal-flow cases it is either minimal or zero. Hence, in our case there is no thin boundary layer near the gas–liquid interface, where the velocity develops, and one may treat it as a single domain problem.

We now determinate the quantitative criteria for the validity of the high Peclet solution. The high Peclet approximation holds when the circulation time, t_c, is much smaller than the characteristic diffusion time, t_d,

$$\frac{t_c}{t_d}<1 \tag{29}$$

The circulation time is defined as:

$$\begin{aligned} t_c&=\oint\frac{\mathrm{d}s_\eta}{h_\eta\upsilon}=\oint\frac{\mathrm{d}\eta}{h_\eta\upsilon},\quad \psi=\text{constant}\\ \upsilon&=\sqrt{(\upsilon_r^2+\upsilon_\theta^2)}=2\kappa\Delta\frac{R}{a^3},\quad \kappa=\frac{9}{160\sqrt{2}}Ba^2\frac{\mu_0}{\mu_l}S^{-1}Re_s^{\frac{1}{2}} \end{aligned} \tag{30}$$

Substituting h_η from Eq. (22) yields after integration, an expression for the circulation time t_c along a streamline ψ.

$$t_c=\frac{A}{\kappa}G(\psi)=\frac{160\sqrt{2}}{9}\left(\frac{a}{B}\right)\left(\frac{\mu_l}{\mu_0}\right)SRe_s^{-\frac{1}{2}}G(\psi) \tag{31}$$

This result indicates that the function $G(\psi)$ has the physical meaning of circulation time along a streamline. Moreover, Eq. (31) relates the circulation time t_c, to the acoustic field parameters, fluid characteristics and droplet size as,

$$t_c \propto \frac{\mu_l}{\mu_0} S Re_s^{-\frac{1}{2}} (A_0 a^2)^{-1} \tag{32}$$

The characteristic diffusion times, with and without reaction are, respectively (Danckwerts, 1951),

$$\tilde{t}_d = \frac{0.056 a^2/D}{1 + \frac{Da}{16}} \tag{33}$$

$$t_d = 0.056 \frac{a^2}{D} \tag{34}$$

the time ratio of the times with and without reaction is:

$$\frac{\tilde{t}_d}{t_d} = \left(1 + \frac{Da}{16}\right)^{-1} \tag{35}$$

Eq. (35) indicates that this ratio decreases as the Da increases.

The validity condition for the high Peclet approximation, Eq. (29), can now be rewritten in terms of $G(\psi)$ as,

$$G(\psi) < 0.0022 Pe Re_s^{\frac{1}{2}} S^{-1} \frac{\mu_0}{\mu_l} \left(1 + \frac{Da}{16}\right)^{-1} \tag{36}$$

While in the absence of reaction $Da = 0$ and the approximation hold when:

$$G(\psi) < 0.0022 Pe Re_s^{\frac{1}{2}} S^{-1} \frac{\mu_0}{\mu_l} \tag{37}$$

We see that criteria for the case of no reaction differ from the criteria with, only by the term containing the Damkoeler number, Da, which represents the intensity of the reaction.

Note from Fig. 3, that the function $G(\psi)$ diverges close to the drop surface, $\psi \to 0$. Thus, there will always be a layer, adjacent to the drop surface, for which the high Peclet assumption is not valid.

As an illustration consider gas absorption from ambient air into a 1-mm water droplet under the influence of a 90-dB, 5 kHz acoustic field. Here, the acoustic field parameters are: $Pe = 350{,}000$, $Re_s = 523$ and $S = 225$. Substitution of these parameters into Eq. (37) indicates that the approximation holds when $G(\psi) < 2.5$, which with the help of Fig. 3 yields $\psi > 0.01$. The region of $\psi < 0.01$ represents a thin layer near the droplet surface. Adding a first order chemical reaction, $k_r = 0.02\,s^{-1}$, to that case we find from Eq. (36) and Fig. 3 that now the approximation holds when $G(\psi) < 1.7$ and $\psi > 0.02$. As seen, here the thickness of the layer in which the approximation does not hold is considerably increased. Hence, we may conclude that the high Peclet approximation holds for cases of no reaction or very slow reaction rates, while the validity of the results for high reaction rates is limited. This statement may be formulated in terms of the relative magnitudes of the Peclet and Damköhler numbers. The solution presented above holds for the case $Pe \gg Da$, and it does not hold for $Pe \leqslant Da$. For cases of arbitrary Peclet numbers, or when $Pe \approx Da$ and $Pe \ll Da$ one has to solve the complete Eq. (11), as outlined below. However, for the case $Pe \ll Da$ the process is controlled by molecular diffusion and chemical reaction,

and the effect of convection is much less important. That case is characterized by a thin concentration boundary layer of the order $O(Da^{-1/2})$.

3.4. Case 3—Absorption into a drop with an arbitrary Peclet number

In this section we present a numerical scheme for the solution of Eq. (11), which describes acoustically enhanced mass transfer into a droplet accompanied by a homogeneous first order chemical reaction.

The time-dependent concentration profile is calculated using an explicit forward finite-difference method in a polar coordinate system. In this method, the known solute concentration profile at time τ is used to calculate the new concentration profile at time $\tau + \Delta\tau$. Hence, the finite-difference equivalent of Eq. (11) is:

$$\begin{aligned} C_{i,j}^{k+1} = {} & C_{i,j}^{k}\left(1 - \frac{2\Delta\tau}{\Delta R^2} - \frac{2\Delta\tau}{R^2\Delta\theta^2} - k_r\Delta\tau\right) + C_{i+1,j}^{k}\left(\frac{\Delta\tau}{\Delta R^2} + \frac{\Delta\tau}{R\Delta R} - \frac{Pe^{*}\upsilon_r\Delta\tau}{4\Delta R}\right) \\ & + C_{i-1,j}^{k}\left(\frac{\Delta\tau}{\Delta R^2} - \frac{\Delta\tau}{R\Delta R} + \frac{Pe^{*}\upsilon_r\Delta\tau}{4\Delta R}\right) C_{i,j+1}^{k}\left(\frac{\cot\theta}{2R^2}\frac{\Delta\tau}{\Delta\theta} + \frac{\Delta\tau}{R^2\Delta\theta^2} - \frac{Pe^{*}\upsilon_\theta\Delta\tau}{4R\Delta\theta}\right) \\ & + C_{i,j-1}^{k}\left(-\frac{\cot\theta}{2R^2}\frac{\Delta\tau}{\Delta\theta} + \frac{\Delta\tau}{R^2\Delta\theta^2} + \frac{Pe^{*}\upsilon_\theta\Delta\tau}{4R\Delta\theta}\right) \end{aligned} \tag{38}$$

The initial and boundary conditions are:

$$\begin{aligned} & C_{n,j} = 1 \quad @\ R = 1, \qquad C_{1,j} = \frac{1}{2}(C_{2,1} + C_{2,m}) \quad @\ R = 0 \\ & C_{i,1} = C_{i,2} \quad @\ \theta = 0 \qquad C_{i,m} = C_{i,m-1} \quad @\ \theta = \frac{\pi}{2} \end{aligned} \tag{39}$$

where i and j are indices defining the angular and radial increments, respectively. The solution domain is a quarter droplet with meshing of 25 radial increments and 22 angular increments and a time step of 1×10^{-5}. Because it was difficult to obtain a stable solution for Peclet numbers greater than 1000, it was necessary to refine the grid for these cases to 40×45 and to reduce the time increment to 1×10^{-6}. We did not notice any influence of the chemical reaction on the stability of the solution.

The mber, Pe^{*}, used in our formulation is a modified Peclet number. It accounts for the oscillation frequency, ω, and velocity amplitude, B, which is related to the acoustic pressure A_0, through Eq. (8). This Peclet number is defined as:

$$\begin{aligned} & Pe^{*} = 0.07955\frac{\mu_0}{\mu_i}Re_s^{-\frac{1}{2}}S^{-1}\,Pe \\ & Pe = \frac{Ba}{D} \end{aligned} \tag{40}$$

The sound pressure is usually measured in dB. Fig. 4 presents how the sound pressure in dB is related to the modified Peclet number, at different frequencies.

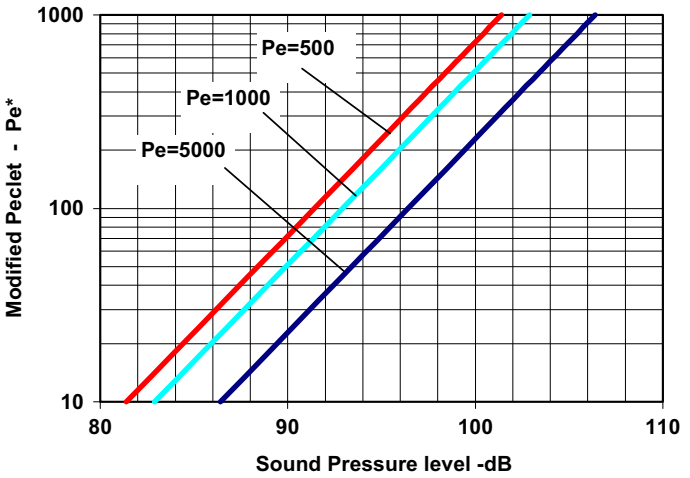

Fig. 4. Relation between the modified Peclet number and the sound pressure for several frequencies.

4. Results

The solution of Eq. (11) yields time dependent concentration profiles. The results are expressed in terms of the following dimensionless variables.

- Average Sherwood number, which represents the instantaneous dimensionless mass transfer rate defined as:

$$Sh_{\text{avg}} = \int_0^{\pi/2} Sh \cdot \sin(\theta)\, \mathrm{d}\theta \tag{41}$$

where Sh, is the local Sherwood number defined as:

$$Sh = 2\frac{\partial C}{\partial R}\bigg|_{R=1} \tag{42}$$

- Average solute concentration

$$C_{\text{avg}} = \frac{1}{V}\int C\, \mathrm{d}V \tag{43}$$

- Time average Sherwood number

$$\langle Sh \rangle = \frac{1}{\tau}\int Sh\, \mathrm{d}\tau \tag{44}$$

The next two sections present the results for absorption with and without chemical reaction for the following range of parameters:

- Modified Peclet numbers of $Pe^* = 0$, 10, 100, 500, 1000, ∞.

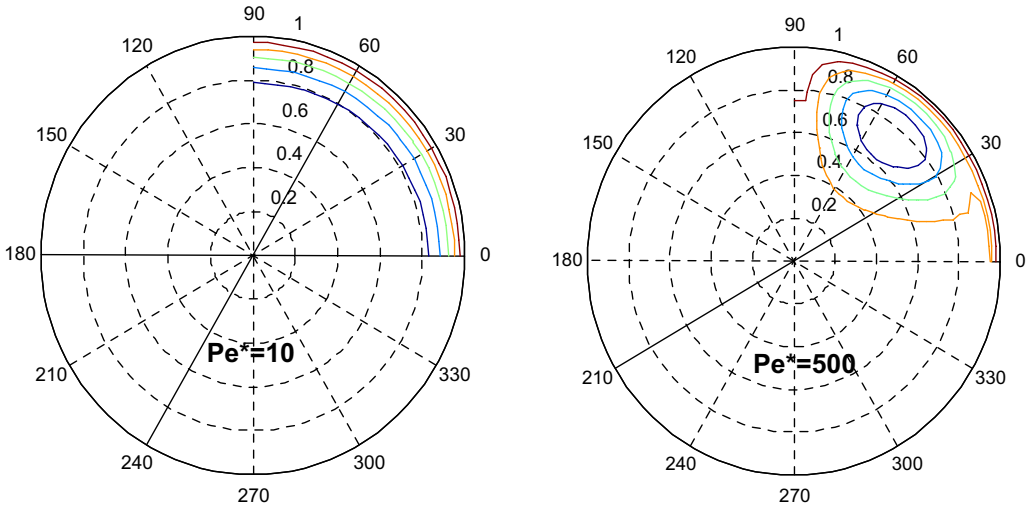

Fig. 5. Effects of modified Peclet numbers on solute concentration inside the droplet for $\tau = 0.02$.

- Dimensionless time, $\tau = 0$–0.1.
- Dimensionless reaction rates, $Da = 0$, 50, 250.

4.1. Mass transfer without chemical reaction

Fig. 5 presents lines of equal solute concentration inside the droplet after $\tau = 0.02$.

Note that for a low intensity acoustic field, which corresponds to a small Peclet number, the lines of equal concentration are concentric and similar to the stagnant drop case. On the other

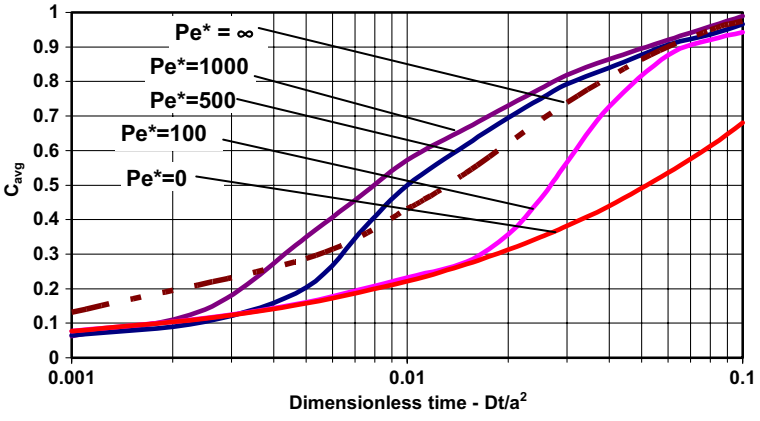

Fig. 6. Time dependent average solute concentration for different Peclet numbers. Solid lines represent the numerical solution. Dashed line is the analytical solution for $Pe^* = \infty$.

hand, for high Peclet numbers the lines of equal concentration coincide with the flow streamlines, see Fig. 1, as found in the high Peclet solution.

Fig. 6 shows the average solute concentration for various Peclet numbers.

For small timescale processes, say $\tau < 0.002$, the diffusion is the dominant mechanism. Thus, the amount of solute does not depend on the Peclet number. For this region it is practically safe to use the simple analytical solution or the Higbie penetration model (Danckwerts, 1970).

Likewise, we see that there is good agreement between the high Peclet solution and the finite-difference one for longer times. The discrepancy between the two models at short times is because the high Peclet analytical solution assumes instantaneous solute distribution along the streamlines. For short times this assumption breaks down. On the other hand, in the finite difference solution, the solute distribution time is accounted for.

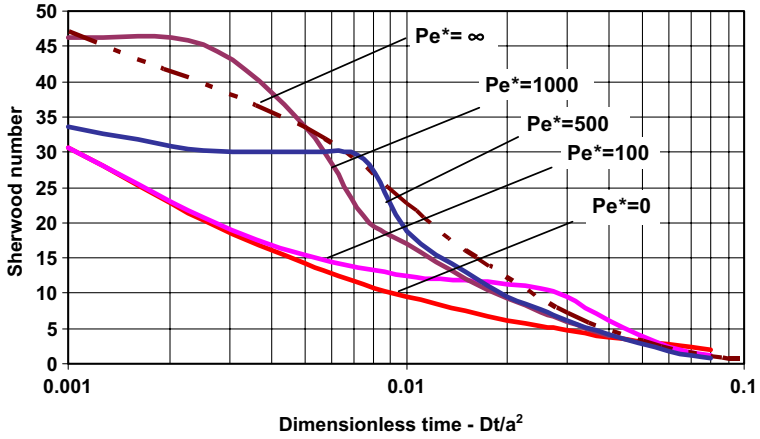

Fig. 7. Time dependent average Sherwood number for different Peclet numbers. Solid lines represent the numerical solution. Dashed line is the analytical solution for $Pe^* = \infty$.

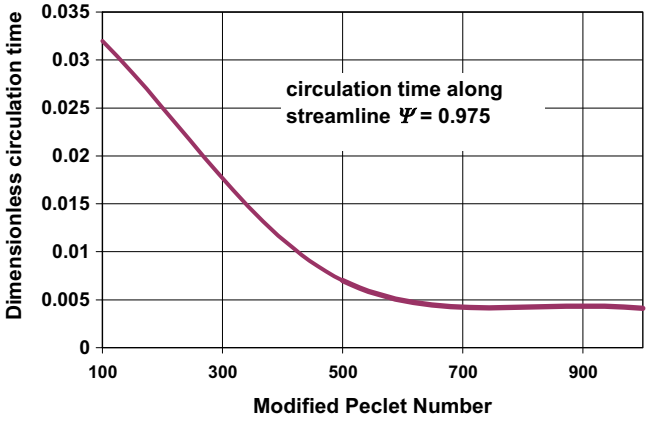

Fig. 8. Circulation time around streamline $\psi = 0.975$ as a function of the modified Peclet number.

For large times, say $\tau > 0.08$ the analytical solution coincides with the numerical results when $Pe^* > 100$.

The changes of the Sherwood number are shown in Fig. 7.

We see that the solution for the Sherwood number from the finite difference scheme tends to fluctuate about the high Peclet solution. Now we assess the relation between the fluctuation frequency of the Sherwood number and the circulation frequency. The timings of these fluctuations correspond to the time required for the circulating liquid to complete a cycle. Fig. 8 presents the time it takes the liquid to complete a cycle for a streamline close to the drop surface, $\psi = 0.975$, for different Peclet numbers.

Thus, we see that for $Pe^* = 500$ the cycle time is 0.007, which corresponds to the appearance of the fluctuation in the Sherwood number in Fig. 7. Watada et al. (1970) predicted similar phenomena of fluctuation in the mass transfer rate in a falling drop.

4.2. Mass transfer with chemical reaction

Fig. 9 presents lines of equal solute concentration inside the drop with and without chemical reaction.

Comparing the shapes of the equal-concentration lines to those of the streamlines in Fig. 1, we see that the deviation of the equal concentration lines from the streamlines is more pronounced when a chemical reaction exists. This can be explained by the dominance of the reaction over convection for short times.

Fig. 10 is similar to Fig. 9, but for longer times. Here, we note that after longer times, the lines of equal concentration without chemical reaction coincide with the streamlines, while with reac-

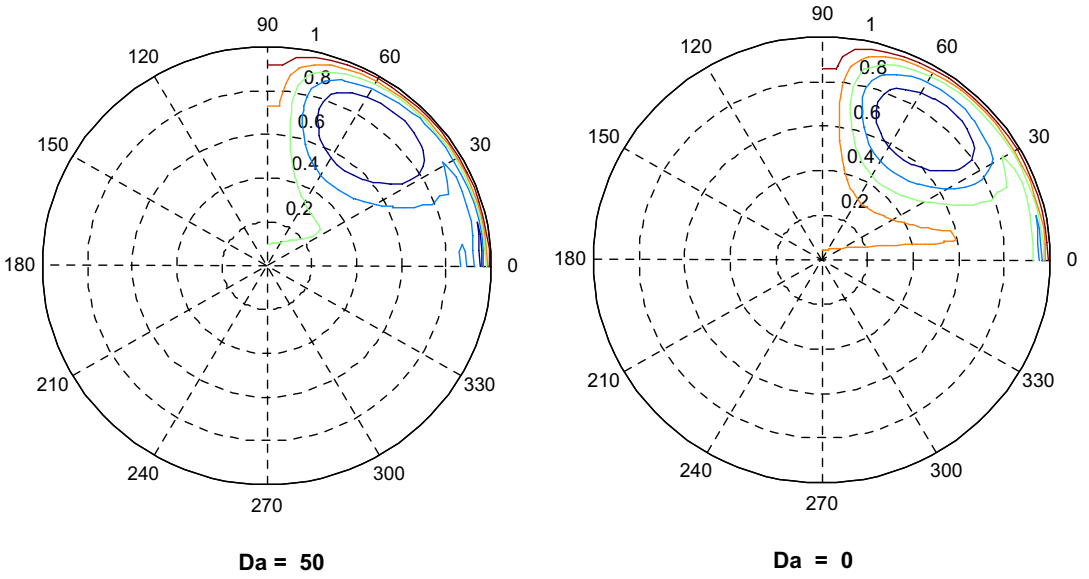

Fig. 9. Effects of reaction rate on the arrangement of equal concentration lines in the drop, $Pe^* = 500$, $\tau = 0.01$.

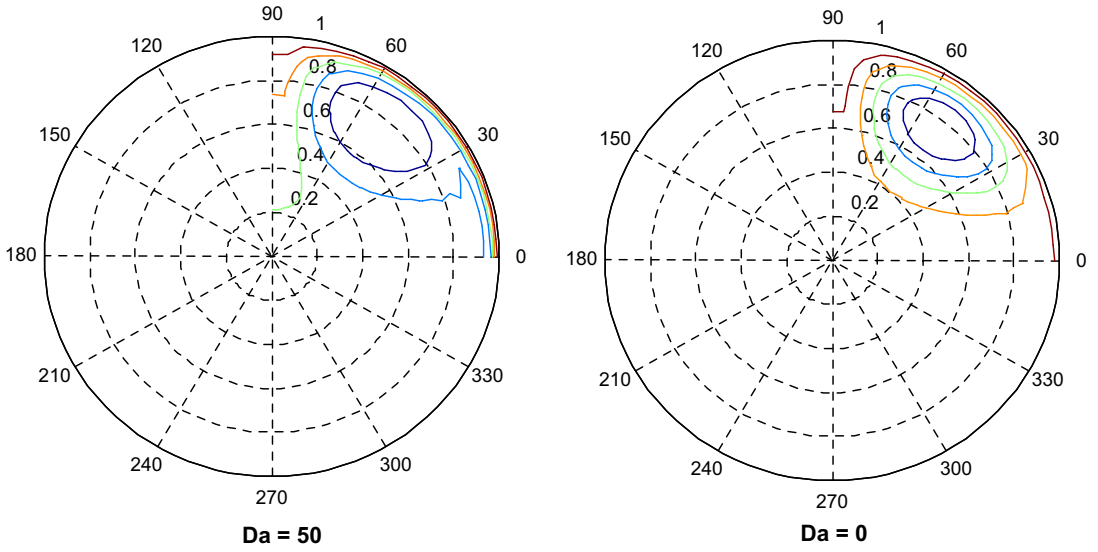

Fig. 10. Effects of reaction rate on the arrangement of equal concentration lines in the drop, $Pe^* = 500$, $\tau = 0.05$.

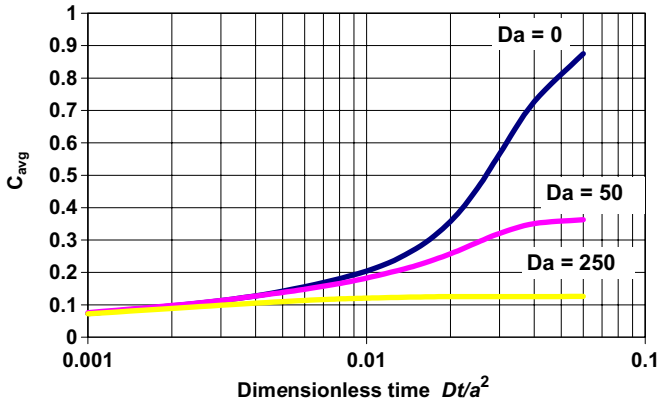

Fig. 11. Dimensionless average solute concentration at different reaction rates for $Pe^* = 100$.

tion they do not. Consequently, while for absorption without reaction, the use of the high Peclet approximation is justified, for absorption with fast chemical reaction it is not.

We now examine the dimensionless parameters characterizing mass transfer into the drop. When mass transfer is accompanied by a first order chemical reaction, the average concentration inside the drop approaches rapidly a constant value. Figs. 11 and 12 present average solute concentrations for Peclet numbers of 100 and 500, respectively.

We see that for a given reaction rate, circulation leads to a significantly higher amount of solute in the drop. Increasing the Peclet number from 100 to 500, almost doubles the amount of ab-

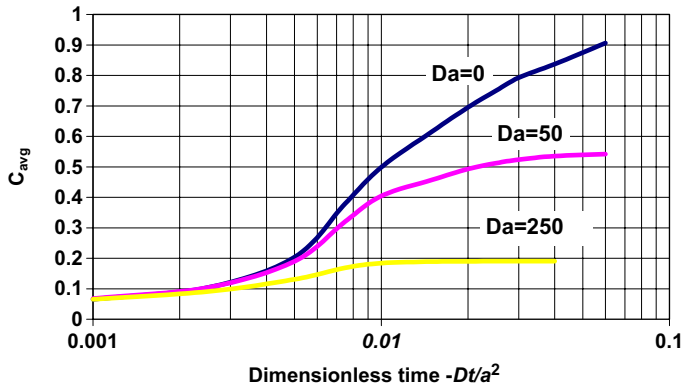

Fig. 12. Average solute concentration at different reaction rates for $Pe^* = 500$.

sorbed gas. Comparing Figs. 11 and 12 we note that for higher circulation rates, i.e. higher Peclet numbers, the approach to constant average concentration is faster.

The dimensionless mass transfer rates given as a Sherwood numbers for Peclet numbers of 100 and 500 are shown in Figs. 13 and 14.

Here again, we may conclude that as the Peclet number increases; so does the instantaneous mass transfer rate.

4.3. Overall mass transfer rate

To gain an indication how acoustics affects the mass transfer process, we now present in Fig. 15 the time average dimensionless mass transfer rate as a function of the modified Peclet number.

We see that for the case of no chemical reaction, $Da = 0$, the high Peclet approximation results practically coincide with the numerical simulation results for $Pe^* > 600$. For the case with chemical reaction, the high Peclet solution slightly overestimates the absorption rate. This is due to the

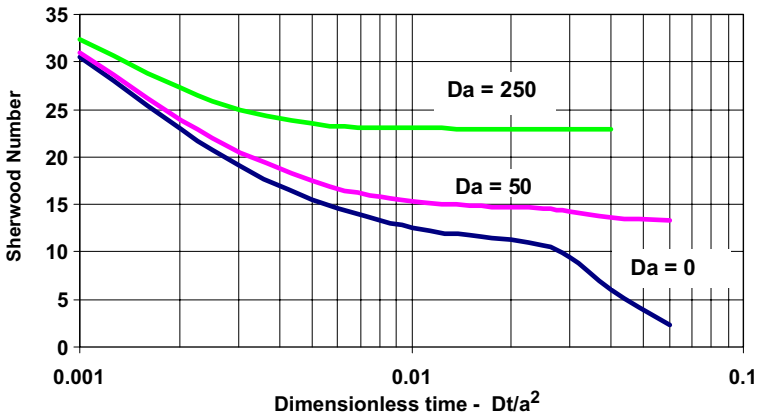

Fig. 13. Dimensionless mass transfer rate at different reaction rates for $Pe^* = 100$.

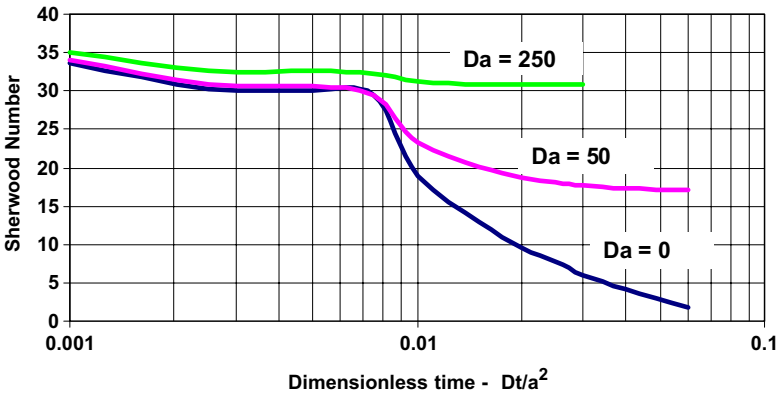

Fig. 14. Dimensionless mass transfer rate at different reaction rates for $Pe^* = 500$.

assumption that the circulation time is much shorter than the diffusion time. The higher the reaction rate the less applicable is the high Peclet solution. Hence, for fast chemical reactions the numerical solution should be used.

In the presence of an acoustic field, the mass transfer rate is enhanced as compared to absorption into a stagnant drop. The enhancement is more evident at low reaction rates. To illustrate this, we present in Fig. 16 the results in the form of an enhancement factor, ϕ which shows the mass transfer enhancement over that into a stagnant drop.

For example for the case of $Pe^* = 500$, which corresponds to a sound pressure of 100 dB and frequency of 1000 Hz, the mass transfer rate is 3.3 times higher than that into a stagnant drop

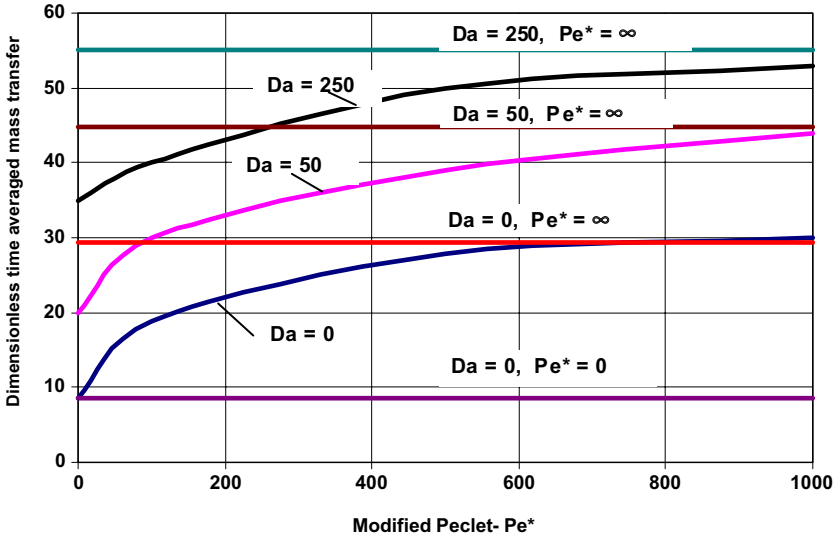

Fig. 15. Time averaged dimensionless mass transfer rate as a function of modified Peclet number for various reaction rates.

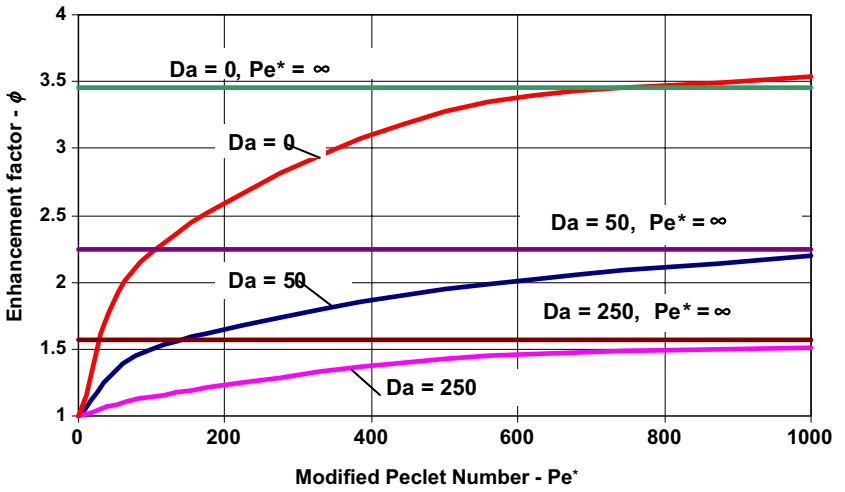

Fig. 16. Time averaged enhancement factor.

without a chemical reaction. For these acoustic conditions with a high rate chemical reaction, the enhancement is only 1.37.

Some experimental works, Larsen and Jensen (1978), correlated mass transfer data in the presence of an acoustic field in terms of exponential relationship between the enhancement factor ϕ and the strength of the acoustic field, as given by the modified Peclet number. In this study the enhancement factor ϕ relates to the modified Peclet number as,

$$\begin{aligned} &\phi \propto \alpha(Pe^*)^n \quad \text{for } 100 < Pe^* < 1000 \\ &0.1 < n < 0.2 \end{aligned} \tag{45}$$

where the value of exponent n depends on the chemical reaction rate and it decreases as the reaction rate increases.

Rewriting this relation using acoustic field parameters A_0 and ω we get,

$$\phi \propto \left(\frac{A_0^2}{\sqrt{\omega}}\right)^n \tag{46}$$

Eq. (46) provides a convenient tool for estimating the enhancement of mass transfer by an acoustic field, of intensity A_0 and frequency ω, as compared to mass transfer without it.

5. Closure

The present work considers acoustically enhanced mass transfer into a liquid drop. Comparing mass transfer rates obtained in the present work, with those of the stagnant drop, we conclude:

1. The effect of acoustic enhancement is important for $Pe^* > 100$, especially for long contact times.
2. For short timescale processes, say $\tau < 0.002$, diffusion controls the mass transfer rate, while convection effects due to acoustic streaming are negligible. Hence, the solute distribution inside the drop is similar to that of a stagnant drop. Here, the familiar models used to describe mass transfer into a stagnant drop can be used.
3. For longer times, say $\tau > 0.08$ and in the absence of chemical reaction, the solution obtained from the high Peclet approximation model may be used when $Pe^* > 600$. For high rate chemical reactions, the validity of the approximation should be carefully assessed using the criteria given in Eq. (36). As shown, high reaction rates reduce the characteristic diffusion time. Consequently, the assumption of a short circulation time is not valid anymore.
4. For cases of intermediate time scales and high reaction rates the finite difference solution has to be used to describe mass transfer.
5. Increasing the modified Peclet number is beneficial for enhancing mass transfer up to $Pe^* = 500$ without chemical reaction and $Pe^* = 1000$ with. Above these values, no additional enhancement was observed.
6. The present work adopted a scheme of single gas absorption into liquid drops accompanied by an irreversible first order reaction. In practice, various industrial processes may involve simultaneous absorption of several gases into the liquid phase. In cases where there is a large dissimilarity between the reaction rates, k_r, of the gases, applying an acoustic field may represent an efficient technique to improve the absorption rate. To demonstrate this, consider the sweetening process of sour natural gas, where CO_2 and H_2S are absorbed into a strong alkaline solution. Here the H_2S absorption is the limiting step of the process, since $Da_{CO_2} \gg Da_{H_2S}$ (Astarita, 1967). Implementing the results of the present work, we may assert that the absorption rate of H_2S, which is characterized by a small Damköhler number, could be improved by applying an acoustic field, while the absorption of CO_2 is not significantly affected (large Damköhler number). Consequently, absorption in the presence of an acoustic field would require a lower contact area as compared to absorption without it.
7. Enhancement of mass transfer into drops by applying an acoustic field is especially attractive for cases without chemical reaction, and should be exploited as a viable industrial process.

References

Andrade, E.N., 1931. On the circulation caused by the vibration of air in a tube. Proc. Roy. Soc. Lond. 134A, 445.

Astarita, G., 1967. Mass Transfer with Chemical Reaction. Elsevier publishing company.

Baxi, C.B., Ramachandran, A., 1969. Effect of vibration on heat transfer from spheres. Trans. ASME J. Heat Transfer, 337–344.

Burdukov, A.P., Nakoryakov, V.E., 1965a. Heat transfer from a cylinder in a sound field at Grashof numbers approaching zero. J. Appl. Mech. Tech. Phys. 6, 112.

Burdukov, A.P., Nakoryakov, V.E., 1965b. On a mass transfer in an acoustic field. J. Appl. Mech. Tech. Phys. 6, 51–55.

Danckwerts, P.V., 1951. Absorption by simultaneous diffusion and chemical reaction into particles of various shapes and into falling drops. Trans. Faraday Soc. 47, 1014–1023.

Danckwerts, P.V., 1970. Gas–Liquid Reactions. McGraw-Hill, New York.

Fyrillas, M., Szeri, A.J., 1994. Dissolution or growth of soluble spherical oscillating bubbles. J. Fluid Mech. 277, 381–407.
Ha, M.Y., Yavuzkurt, S., 1993. A theoretical investigation of acoustic enhancement of heat and mass transfer 1 and 2. Int. J. Heat Mass Transfer 36, 2183–2202.
Kronig, R., Brink, J.C., 1950. On the theory of extraction from falling droplets. Appl. Sci. Res. A2, 142–154.
Lane, C.A., 1956. Acoustical streaming in the vicinity of a sphere. J. Acoust. Soc. Am., 1082–1086.
Larsen, P.S., Jensen, J.W., 1978. Evaporation rates of drops in forced convection with superposed transverse sound field. Int. J. Heat Mass Transfer 21, 511–517.
Lee, C.P., Wang, T.G., 1988. Acoustic radiation force on a heated sphere including effects of heat transfer and acoustic streaming. J. Acoust. Soc. Am. 83, 1324.
Lee, C.P., Wang, T.G., 1989. Near boundary streaming around small sphere due to orthogonal standing waves. J. Acoust. Soc. Am. 85, 1081.
Lemlich, R., Rao, M.A., 1965. The effect of transverse vibration on free convection from horizontal cylinder. Int. J. Heat Mass Transfer 8, 27–33.
Levich, V.G., 1962. Physicochemical Hydrodynamics. Prentice-Hall Inc.
Marthelli, R.C., Boelter, L.M.K., 1939. The effect of vibration on heat transfer by free convection from a horizontal cylinder. In: Proc. 5th Int. Congress of Applied Mechanics, 1939, pp. 578–584.
Mori, Y., Imbayashi, M., Hijikita, K., Yoshuda, Y., 1969. Unsteady heat and mass transfer from spheres. Int. J. Heat Mass Transfer 12, 571–585.
Nasiri, M., Van Moorhem, W.K., 1996. An investigation of heat and mass transfer in oscillating flows at high acoustic Reynolds numbers. Int. Comm. Heat Mass Transfer 23, 613–622.
Raney, W.P., Corelli, J.C., Westervelt, P.J., 1955. Acoustical streaming in the vicinity of a cylinder. J. Acoust. Soc. Am., 1006–1014.
Rhines, P.B., Young, W.R., 1983. How rapidly is a passive scalar mixed within closed streamlines? J. Fluid Mech. 133, 133–145.
Riley, N., 1966. On a sphere oscillation in a viscous fluid. Quart. J. Mech. Appl. Math. 19, 461–472.
Riley, N., 1997. In: M.J. Crocker (Ed.), Acoustic Streaming in Encyclopedia of Acoustics, vol. 1.
Rosenbluth, M.N., Berk, H.L., Doxas, I., Horton, W., 1987. Effective diffusion in laminar convective flow. Phys. Fluids 30, 2636–2647.
Schlichting, H., 1979. Boundary-Layer Theory, seventh ed. McGraw-Hill.
Stone, H.A., Nadim, A., Strogatz, S.H., 1991. Chaotic streamlines inside drops immersed in steady Stokes flows. J. Fluid Mech. 233, 629–646.
Stuart, J.T., 1966. Double boundary layers in oscillatory viscous flow. J. Fluid Mech. 24, 673.
Taylor, F.R.S., 1966. The circulation produced in a drop by an electric field. Proc. Roy. Soc. Lond. 291A, 159–166.
Vainshtein, P., Fichman, M., Gutfinger, C., 1995. Acoustic enhancement of heat transfer between two parallel plates. Int. J. Heat Mass Transfer 38, 1893–1899.
Wang, C.Y., 1965. The flow field induced by oscillating sphere. J. Sound Vibr. 2, 257–269.
Watada, H., Hemielec, A.E., Johnson, A.I., 1970. A theoretical study of mass transfer with chemical reaction in drop. Can. J. Chem. Eng. 48, 225.
Wyllie, C.R., 1995. Advanced Engineering Mathematics, sixth ed. McGraw-Hill, New-York.
Yarin, A.L., Brenn, G., Kastner, O., Rensink, D., Tropea, C., 1999. Evaporation of acoustically levitated droplets. J. Fluid Mech. 399, 151–204.
Yarin, A.L., Kawahara, N., Brenn, G., Kastner, O., Durst, F., 2000. Effect of acoustic streaming on the mass transfer from a sublimating sphere. Phys. Fluids 12, 912–923.
Young, W., Pumir, A., Pomeau, Y., 1989. Anomalous diffusion of tracer in convective rolls. Phys. Fluids 1, 462–469.